

An adaptive safety layer with hard constraints for safe reinforcement learning in multi-energy management systems

Glenn Ceusters^{1,2,3,*} , Muhammad Andy Putratama² , Rüdiger Franke¹, Ann Nowé³ ,
Maarten Messagie² 

¹ ABB, Hoge Wei 27, 1930 Zaventem, Belgium; glenn.ceusters@be.abb.com; ruediger.franke@de.abb.com;

² Vrije Universiteit Brussel (VUB), ETEC-MOBI, Pleinlaan 2, 1050 Brussels, Belgium;
glenn.leo.ceusters@vub.be; muhammad.andy.putratama@vub.be, maarten.messagie@vub.be;

³ Vrije Universiteit Brussel (VUB), AI-lab, Pleinlaan 2, 1050 Brussels, Belgium; gceusters@ai.vub.ac.be;
ann.nowe@ai.vub.ac.be;

* **Correspondence:** glenn.ceusters@be.abb.com

Abstract: Safe reinforcement learning (RL) with hard constraint guarantees is a promising optimal control direction for multi-energy management systems. It only requires the environment-specific constraint functions itself *a priori* and not a complete model (i.e. plant, disturbance and noise models, and prediction models for states not included in the plant model - e.g. demand forecasts, weather forecasts, price forecasts). The project-specific upfront and ongoing engineering efforts are therefore still reduced, better representations of the underlying system dynamics can still be learned and modeling bias is kept to a minimum (no model-based objective function). However, even the constraint functions alone are not always trivial to accurately provide in advance (e.g. an energy balance constraint requires the detailed determination of all energy inputs and outputs), leading to potentially unsafe behavior. In this paper, we present two novel advancements: (I) combining the Optlayer and SafeFallback method, named OptLayerPolicy, to increase the initial utility while keeping a high sample efficiency. (II) introducing self-improving hard constraints, to increase the accuracy of the constraint functions as more data becomes available so that better policies can be learned. Both advancements keep the constraint formulation decoupled from the RL formulation, so that new (presumably better) RL algorithms can act as drop-in replacements. We have shown that, in a simulated multi-energy system case study, the initial utility is increased to 92.4% (OptLayerPolicy) compared to 86.1% (OptLayer) and that the policy after training is increased to 104.9% (GreyOptLayerPolicy) compared to 103.4% (OptLayer) - all relative to a *vanilla* RL benchmark. While introducing surrogate functions into the optimization problem requires special attention, we do conclude that the newly presented GreyOptLayerPolicy method is the most advantageous.

Keywords: reinforcement learning; surrogate optimization; constraints; multi-energy systems; energy management system

Highlights

- Increased initial utility while retaining a high sample efficiency
- Surrogate optimization allows for self-improving hard constraints
- Better policies can be found with more accurate constraints
- Constraint formulation remains decoupled from (optimal) control

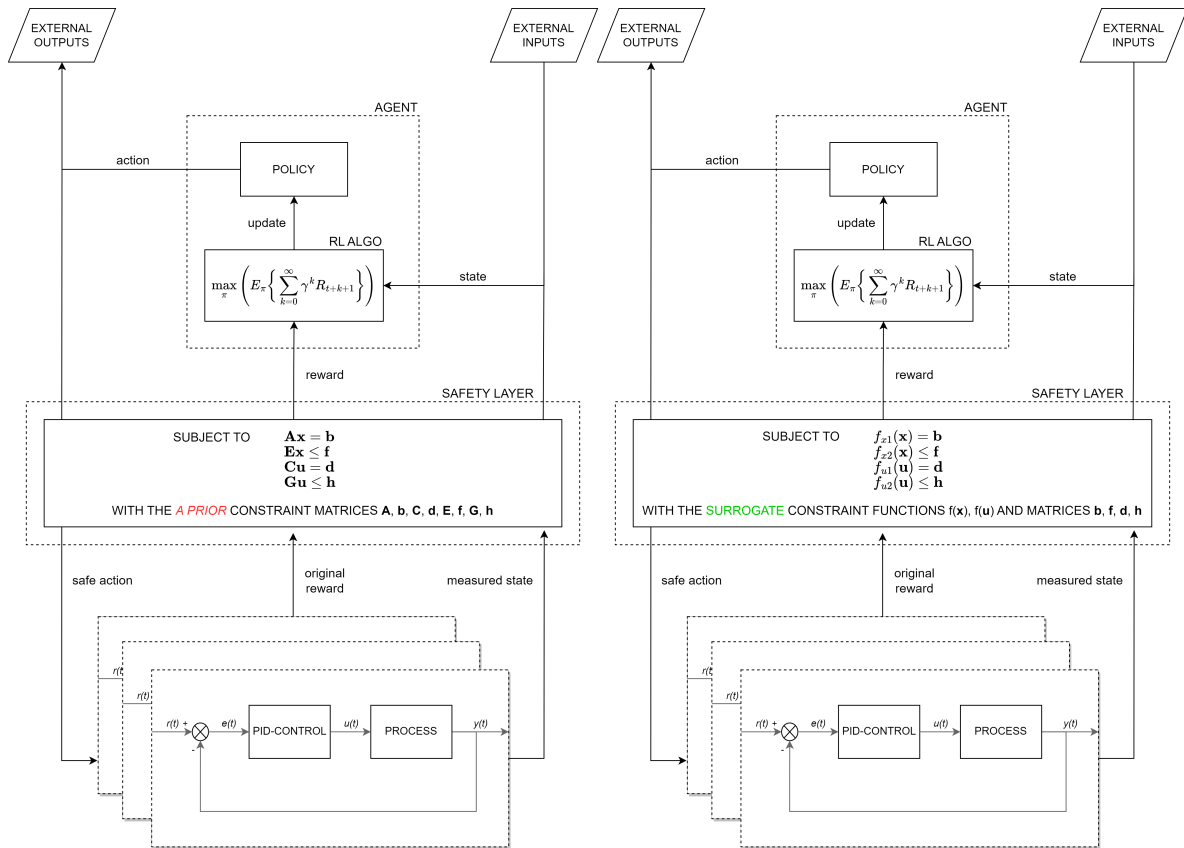
1. Introduction

The possibility to integrate multiple energy, commodity and utility streams is increasingly available as the energy technologies that allow for this sector coupling are more mature, more widely spread deployed and more creatively found. The overall system efficiency and performance can then be enhanced by implementing an integrated control strategy, that considers all energy assets across all energy carriers – including all sources of flexibility (i.e. storage, controllable loads) within all sub-systems. This seemingly limitless optimization potential then typically has an economic or environmental-oriented objective [1] or has a combination of multiple, sometimes conflicting, objectives.

Finding an optimum or Pareto optimum level of operation for such multi-energy systems is no small task. It requires establishing and maintaining specific set-points to firstly ensure a disruptive-free operation by fulfilling all system constraints and secondly to pursue a desired objective (e.g. energy costs or CO₂-equivalent emissions' minimization) [2]. Moreover, the utilization of flexibilities introduces a dependency between successive time steps, which in theory requires an *infinite* horizon optimization calculation. While managing multiple uncertainties (e.g. variation in demands, weather and pricing) only leaves us with an *expectation* in these *continuous* systems.

In practice, model-predictive control (MPC) is often used as the optimal control technique as it has mature stability, feasibility, robustness, and constraint handling theory [3]. However, it does require a detailed model in advance (i.e. plant models, input and output disturbance models, measurement noise models and prediction models for states not included in the plant model – e.g. demand forecasts, weather forecasts, price forecasts) which is typically not adaptive [4]. In an attempt to overcome these shortcomings, reinforcement learning (RL) is model-free and inherently adaptive yet has immature stability, feasibility, robustness, and constraint handling theory. It is only recently that [Ceusters *et al.*](#) [5] showed that a (near-to) optimal multi-energy management policy can be learned safely. Hereby, the project-specific upfront and ongoing engineering efforts remain reduced, a better representation of the underlying system dynamics can still be learned and modelling bias is kept to a minimum (no model-based objective function). However, even the constraint functions themselves (see [Figure 1a](#)) are not always trivial to provide perfectly accurate in advance (e.g. see the energy balance constraint [Equation 9d](#)) – especially when auxiliary state variables are required or when they need to be activated under particular conditions [6].

Our goal, therefore, is not only to ensure that *every* interaction with the underlying environment (a multi-energy system in our case study) is safe by satisfying to a set of constraints. But also to improve the accuracy of the constraints themselves (see [Figure 1b](#)), as more data becomes available, and this with a high initial utility and sample efficiency while the constraint handling remains independent of the (optimal) control technique. This so that future, presumably better, optimization algorithms can act as drop-in replacements.



(a) vanilla shielded (safe) reinforcement learning (b) grey shielded (safe) reinforcement learning

Figure 1. block diagrams comparison: the feasibility of the RL agent's actions, being in a given state, are always checked against a set of either *a priori* or *surrogate* constraint functions acting as a safety layer – shielding the environment from unsafe (control) actions. Note that, we assume that the continuous unconstrained error handling (i.e. minimization of the difference between the desired set-point and a measured process variable) is performed by proportional-integral-derivative (PID) controllers.

1.1. Contribution and outline

Our contributions can, to the best of our knowledge, be listed as the following:

- Combining the Optlayer [6] and SafeFallback [5] method, named OptLayerPolicy, to increase the initial utility while keeping a high sample efficiency.
- Introducing self-improving hard constraints, to increase the accuracy of the constraint functions as more data becomes available so that better policies can be learned.

In [section 2](#) we have a concise related work discussion and formulate our research question, [section 3](#) introduces the proposed methodologies, while [section 4](#) presents the case study specific toolchain, multi-energy system simulation environment, safety layer, RL agent and evaluation procedure. Finally, [section 5](#) discusses the results and provides directions for future work so that [section 6](#) presents our conclusion. In [Appendix A](#) we show time series visualizations of the different policies, in [Appendix B](#) the full learning and cost curves for the assessed agents in the case study, in [Appendix C](#) the pseudocode of the specific RL agent (TD3) and in [Appendix D](#) the run-time statistics.

2. Related work

Reinforcement learning has been proposed and demonstrated for a wide variety of applications in power and energy systems, as extensively reviewed by e.g. [Cao et al. \[7\]](#), [Yang et al. \[8\]](#) and [Perera and Kamalaruban \[9\]](#), and even for multi-energy systems more specifically by [Zhou \[10\]](#). It ranges from real-time control (e.g. robust voltage control by [Petrusev et al. \[11\]](#)) to energy management systems (EMS) RL applications. Recent EMS examples include, [Zhou et al. \[12\]](#) who proposed deep RL for the stochastic EMS of a multi-energy system and introduced a prioritized experience relay that improves the training efficiency and thus the convergence rate of the RL algorithm. While a multi-agent deep RL EMS, using multi-agent counterfactual soft actor-critic (mCSAC [13]), was demonstrated by [Zhu et al. \[14\]](#) on a simulated multi-energy industrial park, by [Ahrarinouri et al. \[15\]](#) using multi-agent Q-learning on a simulated distributed and interconnected multi-carrier energy hub case study, and by [Jendoubi and Bouffard \[16\]](#) using multi-agent Deep Deterministic Policy Gradient (MADDPG) on separate simulated microgrid, eco-neighborhood and flat building case studies. [Ceusters et al. \[4\]](#), furthermore, benchmarked an on- and off-policy multi-objective model-free deep RL algorithm against a linear MPC on two separate simulated multi-energy systems and showed that the RL agent, using soft constraints, can outperform the MPC (as it learned a better representation of the *true* system dynamics). [Sun et al. \[17\]](#) then also demonstrated a multi-objective deep RL approach with soft constraints yet on an IEEE-30 node optimal power flow problem. [Ceusters et al. \[5\]](#) then were one of the first to show that a (near-to) optimal multi-energy management policy can be learned safely with hard constraints, that these constraints can be formulated independently of the (optimal) control technique and that better policies can be found starting from an initial safe fallback policy. While [Feng et al. \[18\]](#) introduced a robust state generation procedure in combination with a dynamic pricing mechanism to economically dispatch an industrial park using a variation of the distributed proximal policy optimization (DPPO) algorithm subject to a set of hard constraints to ensure safe (near-to) optimal operation. However, even only assuming the availability of perfectly accurate constraint functions themselves is not always possible – especially when auxiliary state variables are required or when they need to be activated under particular conditions, as also needed by `OptLayer` [6] which [Ceusters et al. \[5\]](#) used as a benchmark.

Considering a broader view across both the RL research space and the control theory space, [Brunke et al. \[19\]](#) provided a safe learning review and showed: (1) approaches that learn uncertain system dynamics and safely improve the policy starting with an imperfect *a priori* dynamic model, (2) approaches that don't have a model or even constraints in advance and encourage safety or robustness (e.g. by penalizing dangerous actions) but provide no strict guarantees, and (3) approaches that provide safety certificates to inherently unsafe learning-based controllers, using an *a priori* dynamic model. Hence, multiple safe (reinforcement) learning approaches exist, ranging in level of safety namely (from lower to higher level): soft-constraint satisfaction, chance-constraint satisfaction and hard-constraint satisfaction. Recent examples – one of each category – include, [McKinnon and Schoellig \[20\]](#) who proposed a stochastic MPC, where the predicted cost, using a computationally efficient yet expressive-limited *a priori* dynamic model, is corrected by a simple learned dynamics model over the MPC horizon. [Bharadhwaj et al. \[21\]](#) who extended Conservative Q-Learning

(CQL) towards Conservative Safety Critic (CSC) and showed safety constraint satisfaction with *high probability* while providing provable safe policy improvements. And finally, [Lopez et al. \[22\]](#) who introduced robust adaptive control barrier functions (CBF) which allowed safe adaptation of structured parametric uncertainties in the time derivatives of CBFs which is used together with an inherently unsafe adaptive control algorithm.

Nevertheless, a model-free safe RL approach of the following *combined* characteristics has – to the best of our knowledge – never been proposed: (i) providing hard-constraints satisfaction guarantees (ii) while decoupled from the RL (as a Markov Decision Process) formulation, (iii) both during training a (near) optimal policy (which involves exploratory and exploitative steps) as well as during the deployment of any policy (e.g. random agents or offline pre-trained RL agents) and (iv) this while learning uncertain constraint components and safely improving the policy with high sample efficiency, and (v) starting from an increased initial utility, to (vi) demonstrate for the energy management of multi-energy systems.

3. Proposed methodology

We start from a discrete time-varying stochastic system and acknowledge this is an approximation for continuous¹ systems, in the form of:

$$x_{t+1} = f_t(x_t, u_t, w_t) \quad (1)$$

where x_t is the n -dimensional *state* vector, which is an element of the *state space* \mathbb{X} , and u_t the m -dimensional *control* or *action* vector, which is an element of the input or *action space* \mathbb{U} , and w_t a Wiener process, i.e. some stochastic noise, that – with this formulation – can enter the dynamics in any form. The problem is to find a control signal $u_t = \pi_t(x_t)$, with π being the control *policy*, so that the infinite-horizon, yet discounted (if $\gamma^t < 1$), cost function

$$C(x_i, u_t) = E \left\{ \sum_{t=0}^{\infty} \gamma^t L_t(x_t, u_t, w_t) \right\} \quad (2)$$

is minimal, where $L_t(x_t, u_t, w_t)$ is the stage *loss*. Given the stochastic nature of the considered system ([Equation 1](#)), one can only hope to minimize the *expectation* $E\{\cdot\}$ of this cost function over all stochastic trajectories that start in x_i . This results in the discounted infinite-horizon objective function:

$$J_{\infty}(x_t) = \min_{u_t \in \mathbb{U}_t} \left(E \left\{ \sum_{t=0}^{\infty} \gamma^t L_t(x_t, u_t, w_t) \right\} \right), \forall x_t \quad (3)$$

Following the standard RL formulation of the state-value function, the objective is to find a policy π , which is a mapping of states, $s = x$, to actions, $a = u$, that maximizes an expected sum of discounted rewards, yet making it subject to the constraints, c :

¹ as we assume that the continuous error handling is performed by well-tuned PID-controllers

$$\max_{\pi} \left(E_{\pi} \left\{ \sum_{k=0}^{\infty} \gamma^k R_{t+k+1} \right\} \right) \quad (4a)$$

$$s.t. \quad s_t = s \quad t \in \mathbb{T}_0^{+\infty} \quad (4b)$$

$$c_t^j(s_t, a_t, w_t) \leq 0 \quad t \in \mathbb{T}_0^{+\infty}, j \in \mathbb{R}_1^{n_c} \quad (4c)$$

where E_{π} is the expected value, following the policy π , of the rewards R and reduced with the discount factor γ over an infinite sum at any time step t with n_c amount of constraint functions.

Note that [Equation 4a](#) is a discrete time-invariant infinite-horizon stochastic optimal control problem, i.e. the time-invariant version of [Equation 3](#) (as $R_t = -L_t(x_t, u_t, w_t)$), yet differs from the standard formulation of RL due to the hard-constraint functions subjection c_t^j . This can include *state constraints* $\mathbb{X}_c \in \mathbb{X}$, action or *input constraints* $\mathbb{U}_c \in \mathbb{U}$ and *stability guarantees* (e.g. Lyapunov, asymptotic or exponential stability). Rather than proposing a specific safe RL algorithm, we propose to decouple the constraint function formulation from the (RL) agent so that any (new RL) algorithm can be used – while always guaranteeing hard-constraint satisfaction and this in a minimally invasive way (i.e. correcting actions to the closest possible feasible action).

3.1. OptLayerPolicy method

The minimal invasive correction of predicted actions, \tilde{a} , e.g. originating from a RL algorithm, can be expressed as:

$$a_{safe,t} = \arg \min_{a_t} \frac{1}{2} \| a_t - \tilde{a}_t \|^2 \quad (5a)$$

$$s.t. \quad c_t^j(s_t, a_t, w_t) \leq 0 \quad t \in \mathbb{T}_0^{+\infty}, j \in \mathbb{R}_1^{n_c} \quad (5b)$$

which is a Quadratic Program (QP), similar to the OptLayer [\[6\]](#) algorithm. The distance closest to the possible feasible action is then simply:

$$d_{safe,t} = \min_{a_t \in \mathbb{R}^{n_c}} \frac{1}{2} \| a_t - \tilde{a}_t \|^2 \quad (6)$$

While this is the closest distance for a minimally invasive correction, this does not necessarily result in a close-to-optimal action. We, therefore, propose to fallback on an *a priori* safe policy, π^{safe} (i.e., use the SafeFallback [\[5\]](#) algorithm), when the distance, d_{safe} , surpasses a given threshold. While this relies on the utility of the (non-optimal) safe fallback policy itself, we will later show its effectiveness. The OptLayerPolicy algorithm is shown in [algorithm 1](#).

3.2. GreyOptLayerPolicy method

We can improve the initial utility of the *vanilla* RL agent, by using a safe fallback policy when a predicted unsafe action is too far from the feasible solution space (i.e. under the notion

Algorithm 1: OptLayerPolicy

```

1 Input: initialize RL algorithm, initialize constraint functions in sets  $\mathbb{X}_c$  and  $\mathbb{U}_c$ ,
   initialize safe fallback policy  $\pi^{safe}$ 
2 for  $k = 0, 1, 2, \dots$  do
3   Observe state  $s$  and predict action  $\tilde{a}$ 
4   Compute safety distance  $d_{safe}$ 
5   if  $d_{safe} \leq h_{safe}$  then
6      $a_{safe} = \arg \min_{a_t \in \mathbb{R}^{n_c}} \frac{1}{2} \| a_t - \tilde{a}_t \|^2$ 
7   else
8      $a_{safe} = \pi^{safe}(s)$ 
9   end
10  Execute  $a_{safe}$  in the environment
11  Observe next state  $s'$ , reward  $r$  and done signal  $d$  to indicate whether  $s'$  is terminal
12  Give experience tuple  $(s, a_{safe}, r, s', d)$  and if  $a_{safe} \neq \tilde{a} : (s, \tilde{a}, r - z, s', d)$  with cost  $z$ 
13  If  $s'$  is terminal, reset environment state
14 end

```

that random² safe actions have a low utility). However, all constraint functions (Equation 5b) are assumed to be *true*. In reality, we typically only have access to a nominal set of constraints with an *a priori* unknown error (e.g. see Equation 9d and Table 2). We can express this as:

$$c_t^j(s_t, a_t, w_t) = \bar{c}_t^j(s_t, a_t) + \hat{c}_t^j(s_t, a_t, w_t) \quad (7)$$

where $(\bar{\cdot})$ is the nominal component, reflecting our prior knowledge, and $(\hat{\cdot})$ an unknown component, that can be learned from data. The GreyOptLayerPolicy algorithm is exactly the same as the previous method, yet where Equation 5b is replaced by Equation 7. However, this does introduce function approximators (e.g. artificial neural networks) into the optimization problem (Equation 5a) – which are not trivial to integrate when using exact solving methods (e.g. Gunnell *et al.* [23] only recently integrated multiple machine learning algorithms in a gradient descent optimization framework).

4. Case study

4.1. Toolchain

We use a multi-energy systems simulation model, that first was developed by Ceusters *et al.* [4] and later modified by Ceusters *et al.* [5]. This allowed for the consequence-free verification of the safe operation (i.e. with no risk of violating real-life constraints with its potential loss of comfort or, in extreme cases, human harm). The presumed to be *true* multi-physical first-principle equations were developed in Modelica [24] due to its object-oriented nature and the availability of highly specialized libraries and elementary components. To allow for the exchange across different simulation environments and

² as RL agents typically have an initial random exploration phase

programming languages, this dynamic system model was exported as a co-simulation *functional mock-up unit* (FMU), as also proposed by Gräber *et al.* [25] and then wrapped in an OpenAI gym [26] in Python. The mixed-integer quadratic problem in the safety layer was formulated with GEKKO [27], as it allowed for the integration of machine learning algorithms (used for $\hat{\cdot}$) in Equation 7) into an exact optimization framework. The tool-chain architecture is shown in Figure 2.

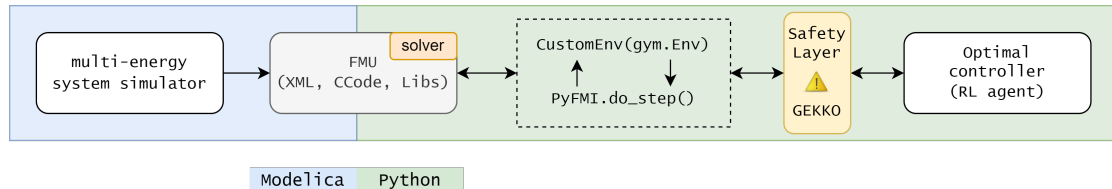


Figure 2. Architecture of the tool-chain. Note that the Differential Algebraic Equations’ solver is part of the co-simulation FMU and that the `do_step()` method in PyFMI [28] is used over `simulate()` – due to the significant run-time speed-up when initialized properly.

4.2. Simulation model

The simulated multi-energy system, from Ceusters *et al.* [5], has the following structure:

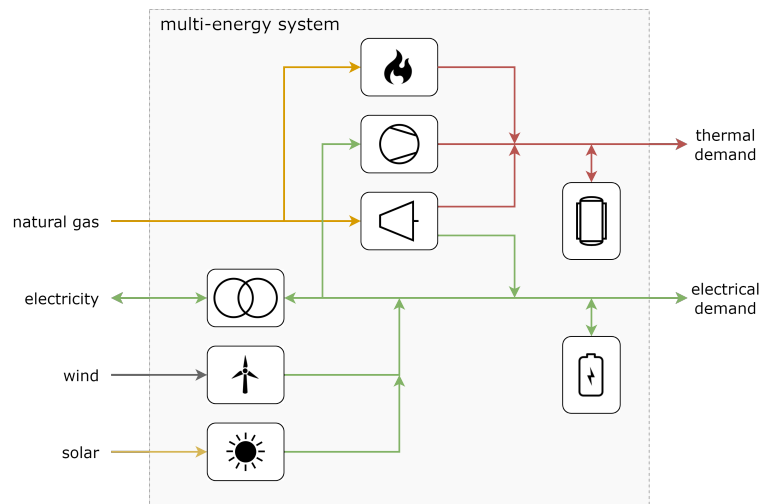


Figure 3. Structure of the simulated multi-energy system.

It includes (from left to right, from top to bottom): an electric grid connection, a wind turbine, a photovoltaic (PV) installation, a natural gas boiler, a heat pump (HP), a combined heat and power (CHP) unit, a thermal energy storage system (TESS) and a battery energy storage system (BESS). The dimensions of the considered multi-energy system are summarised in Table 1.

As also reported by Ceusters *et al.* [5], the simulation model is a detailed system of differential-algebraic equations (2.548 equations with an equal amount of variables). However, it does not include any simulated control system (e.g. including PID controllers). While we acknowledge the simplification, we make an abstraction of this control layer for this case study. The resulting control error is approximately 5%, as determined by Ceusters *et al.* [5] with separate simulations using a reduced discrete-time control horizon (5 seconds compared

Table 1. Dimensions of the multi-energy system.

Energy asset	Input	Output	P_{nom}	P_{min}	E_{nom}
grid connection	elec	elec	$+\infty$	$-\infty$	
wind turbine	wind	elec	0.8 MW_e	1.5 %	
solar PV	solar	elec	1.0 MW_e	0 %	
boiler	CH_4	heat	2.0 MW_{th}	10 %	
heat pump	elec	heat	1.0 MW_{th}	25 %	
CHP	CH_4	heat	1.0 MW_{th}	50 %	
	CH_4	elec	0.8 MW_e	50 %	
TESS	heat	heat	$+0.5 \text{ MW}_{th}$	-0.5 MW_{th}	3.5 MWh
BESS	elec	elec	$+0.5 \text{ MW}_e$	-0.5 MW_e	2.0 MWh

to 15 minutes, without any continuous *error* handling). This assumption is the same for every considered energy management algorithm, so the comparison remains valid.

4.3. Safety layer

Starting from minimum and maximum electrical and thermal power output constraints:

$$Q_{boil}^{min} \times \gamma_{boil}^t \leq Q_{boil}^t \leq Q_{boil}^{max} \times \gamma_{boil}^t \quad \forall t, \gamma_{boil}^t \in \{0, 1\} \quad (8a)$$

$$\begin{bmatrix} Q_{hp}^{min} \\ P_{hp}^{min} \end{bmatrix} \times \gamma_{hp}^t \leq \begin{bmatrix} Q_{hp}^t \\ P_{hp}^t \end{bmatrix} \leq \begin{bmatrix} Q_{hp}^{max} \\ P_{hp}^{max} \end{bmatrix} \times \gamma_{hp}^t \quad \forall t, \gamma_{hp}^t \in \{0, 1\} \quad (8b)$$

$$\begin{bmatrix} Q_{chp}^{min} \\ P_{chp}^{min} \end{bmatrix} \times \gamma_{chp}^t \leq \begin{bmatrix} Q_{chp}^t \\ P_{chp}^t \end{bmatrix} \leq \begin{bmatrix} Q_{chp}^{max} \\ P_{chp}^{max} \end{bmatrix} \times \gamma_{chp}^t \quad \forall t, \gamma_{chp}^t \in \{0, 1\} \quad (8c)$$

$$Q_{tess}^{min} \leq Q_{tess}^t \leq Q_{tess}^{max} \quad \forall t \quad (8d)$$

$$P_{bess}^{min} \leq P_{bess}^t \leq P_{bess}^{max} \quad \forall t \quad (8e)$$

where Q^t and P^t are the thermal and electrical powers respectively (in accordance with Table 1) and γ^t binary variables that turn on/off the given asset (i.e. as their minimal powers are not zero). Furthermore, we assume a sufficiently large grid connection so that the electrical energy balance is always fulfilled. By doing so, we focus on satisfying the thermal energy balance and no additional constraints are considered in this case study (e.g. minimal run- and downtime, ramping rates). Writing out the thermal energy balance then becomes:

$$Q_{production}^t = Q_{demand}^t \quad \forall t \quad (9a)$$

$$Q_{boil}^t + Q_{hp}^t + Q_{chp}^t + Q_{tess}^t = Q_{demand}^t \quad \forall t \quad (9b)$$

$$a_{boil}^t \cdot \eta_{boil}^t \cdot Q_{boil}^{max} + a_{hp}^t \cdot \frac{COP_{hp}^t}{COP_{hp}^{max}} \cdot Q_{hp}^{max} + a_{chp}^t \cdot \eta_{chp}^{t,th} \cdot Q_{chp}^{max} + a_{tess}^t \cdot f(SOC_{tess}^t) = Q_{demand}^t \quad \forall t \quad (9c)$$

$$a_{boil}^t \cdot f(T_{boil}^t) \cdot Q_{boil}^{max} + a_{hp}^t \cdot \frac{f(T_{evap}^t, T_{cond}^t)}{COP_{hp}^{max}} \cdot Q_{hp}^{max} + a_{chp}^t \cdot f(P_{chp}^t, Q_{chp}^t, T_{env}^t) \cdot Q_{chp}^{max} + a_{tess}^t \cdot f(\overline{T}_{tess}^t) = Q_{demand}^t \quad \forall t \quad (9d)$$

where a are the (control) actions, η the energy efficiencies, COP the coefficient of performance, SOC the state of charge, and T various specific temperatures (i.e. T_{boil}^t the return temperature to the boiler, T_{evap}^t the evaporator temperature of the heat pump, T_{cond}^t the condenser temperature of the heat pump, T_{env}^t the environmental air temperature and $\overline{T_{tess}^t}$ the average temperature in the stratified hot water storage tank). However, the different functions $f(\cdot)$ from Equation 9d are typically not trivial to *model* accurately. Our nominal models ($\bar{\cdot}$) in Equation 7, which are also the ones used in Equation 5b, have the following metrics:

Table 2. Safety layer: nominal modelling metrics. Mean Absolute Error (MAE), Normalised Mean Absolute Error (NMAE) by range, i.e. $NMAE = MAE / \text{range}(\text{actual values})$

Energy asset	R2-score	MAE	NMAE
boiler	99.70%	20.00 kW	0.90%
heat pump	97.05%	36.04 kW	3.64%
CHP	99.77%	4.20 kW	0.35%
TESS	85.64%	39.52 kW	4.18%

In our nominal models we have assumed a linear time-invariant relationship between the (control) action and the thermal power for the boiler and the CHP, yet a 3rd-degree polynomial for the TESS and a 2nd-degree polynomial for the heat pump – both also time-invariant. We note from Table 2 that the main improvement can be made in the heat pump and thermal energy storage functions and that we use the *a priori* safe fallback policy π^{safe} from Ceusters *et al.* [5] - which is a simple priority/cascading rule.

4.4. Energy managing RL agent

We formulate the energy managing RL agent as a fully observable discrete-time Markov Decision Process (MDP) with the tuple $\langle S, A, P_a, R_a \rangle$ so that:

$$S^t = (E_{th}^t, E_{el}^t, P_{wind}^t, P_{solar}^t, X_{el}^t, SOC_{tess}^t, SOC_{bess}^t, h^t, d^t) \quad S^t \in S \quad (10a)$$

$$a_{boil}^t = (0, a_{boil}^{min} \rightarrow a_{boil}^{max}) \quad a_{boil}^t \in A \quad (10b)$$

$$a_{hp}^t = (0, a_{hp}^{min} \rightarrow a_{hp}^{max}) \quad a_{hp}^t \in A \quad (10c)$$

$$a_{chp}^t = (0, a_{chp}^{min} \rightarrow a_{chp}^{max}) \quad a_{chp}^t \in A \quad (10d)$$

$$a_{tess}^t = (a_{tess}^{min} \rightarrow a_{tess}^{max}) \quad a_{tess}^t \in A \quad (10e)$$

$$a_{bess}^t = (a_{bess}^{min} \rightarrow a_{bess}^{max}) \quad a_{bess}^t \in A \quad (10f)$$

$$R_a = -(x \times L_{cost}^t + y \times L_{comfort}^t) - z \quad (10g)$$

where E_{th}^t is the thermal demand, E_{el}^t the electrical demand, P_{wind}^t the electrical wind in-feed, P_{solar}^t the electrical solar in-feed, X_{el}^t the electrical price signal, SOC_{tess}^t the state-of-charge (SOC) of the TESS, SOC_{bess}^t the SOC of the BESS, h^t the hour of the day and d^t the day of the week all at the t -th step, which constitute the state-space S . The action space A includes the control set-points from, a_{boil}^t the natural gas boiler, a_{hp}^t the heat pump, a_{chp}^t the CHP unit,

$a_{t_{\text{tess}}}^t$ the TESS, and $a_{t_{\text{bess}}}^t$ the BESS all between the minimum and maximum power rates in accordance with [Table 1](#).

We formulate the objective, i.e. the reward function, so that when maximizing this function (via [Equation 4a](#)) we minimize the positive version of that function. Hence, we minimize the energy costs L_{cost}^t in EUR and the loss in (thermal) comfort $L_{\text{comfort}}^t = |Q_{\text{demand}}^t - Q_{\text{production}}^t|$ in Watt with scalarisation weights $x = 1/10$ and $y = 1/5e5$ and with an additional cost $z = 1$ to further shape the reward when the original, uncorrected, predicted action \tilde{a} was *expected* to violate the constraints. The loss in (thermal) comfort, L_{comfort}^t , serves as an additional fine-tuning mechanism to further mitigate the modelling error of the constraints itself (see [Table 2](#)), i.e. to additionally shape the reward and thus guide the agent towards safer actions. The discrete-time control horizon is 15 minutes. The state-space S is normalized and all actions in the action-space A are scaled between $[+1, -1]$.

As the specific RL algorithm, we use a twin delayed deep deterministic policy gradient (TD3) agent from the `stable` baseline [\[29\]](#) implementations. The pseudocode of the TD3 algorithm is given in [Appendix C](#) and we have the following hyperparameters.

Table 3. TD3 hyperparameters. The parameters from the *vanilla* Unsafe agent are the result of an optimization study from [Ceusters et al. \[4\]](#), while the others are the resulting SafeFallback parameters from [Ceusters et al. \[5\]](#)

Hyperparameters: TD3	Unsafe	OptLayer	OptLayerPolicy	GreyOptLayerPolicy
gamma	0.9	0.7	0.7	0.7
learning_rate	0.0003833	0.000583	0.000583	0.000583
batch_size	100	16	16	16
buffer_size	1e5	1e6	1e6	1e6
train_freq	2e3	1e0	1e0	1e0
gradient_steps	2e3	1e0	1e0	1e0
noise_type	normal	normal	normal	normal
noise_std	0.329	0.183	0.183	0.183

4.5. Evaluation

We evaluate our methods, `OptLayerPolicy` and `GreyOptLayerPolicy`, against a *vanilla* RL agent (i.e. without a safety layer and therefore being unsafe), the original `OptLayer` from [Pham et al. \[6\]](#) and the original `SafeFallback` from [Ceusters et al. \[5\]](#), on a week-long evaluation environment while having a separate year-long training environment using the simulation model as discussed in [subsection 4.2](#). This, in terms of energy costs minimization subject to constraint fulfilment (i.e. all RL agents have the same [Equation 10g](#)). We also include random agents, to further study the effectiveness of the safety layers and to serve as a minimal learning benchmark. The linear MPC from [Ceusters et al. \[4\]](#) is not included here, as the constraints can be formulated directly in the method. Note that, any uncertainty (e.g. from demands, prices, or renewables) is inherently handled by the RL agents in accordance with the *expectation* $E\{\cdot\}$ in [Equation 4a](#).

5. Results and discussion

The simulated performance, in terms of energy cost minimization subject to constraint fulfilment, is shown in [Table 4](#) and [Table 5](#). The objective values (i.e. the rewards) are

shown both in absolute values (using Equation 10g) and relative to the *vanilla* RL benchmark (i.e. without a safety layer). The constraint tolerance, we define here as the difference between the *true* constraints (i.e. observed after executing the control actions in the simulation environment) and the *modelled* constraints in the safety layer (i.e. computed in the safety layer itself, which is only *believed* to be true – see Table 2 and Figure 6). While, in principle, this is a calculation for the complete constraint set, we focus here on the most limiting constraint being the thermal energy balance of Equation 9d. Note that, this is only for the constraint tolerance metric and that Equation 8a till Equation 8e are still part of the mixed-integer quadratic program in the safety layer (this as their influence on the metric over the complete constraint set is marginal and can therefore be neglected). The constraint tolerance metric is then shown as the mean average error normalized to the range of the thermal demand (NMAE) and shown as the normalized sum (NSUM) over all evaluation time steps (i.e. 0% would then mean, perfect thermal energy balance and thus constraint fulfilment over all evaluation time steps). We again want to emphasize the lack of a simulated control system (as discussed in subsection 4.2), resulting in an NSUM of approximately 5%, as determined by Ceusters *et al.* [5] on the same simulated case study.

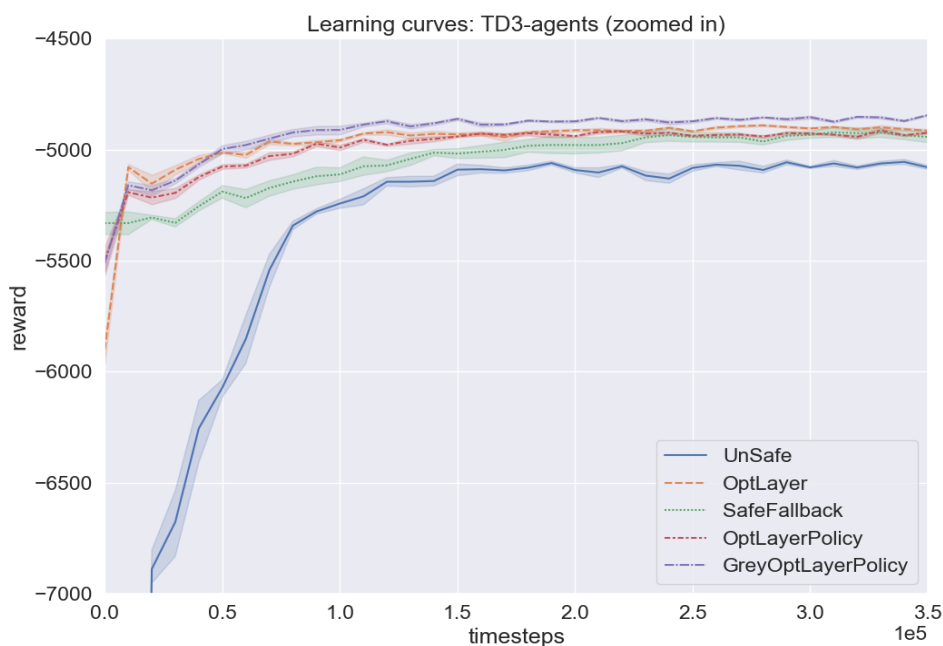
Table 4. 5-run average policy performance with a training budget of 10 years worth of time steps per run (i.e. 350,400 time steps per run)

EMS algorithm	Objective value		Constraint tolerance	
	absolute	relative	NMAE	NSUM
Unsafe TD3	-5,080	100.0%	8.1%	22.3%
OptLayer TD3	-4,915	103.4%	2.3%	6.1%
SafeFallback TD3	-4,943	102.8%	3.9%	9.9%
OptLayerPolicy TD3	-4,924	103.2%	2.4%	6.2%
GreyOptLayerPolicy TD3	-4,844	104.9%	2.5%	6.5%

These results (Table 4 and Table 5) show that our GreyOptLayerPolicy method outperforms all other benchmarks after training (104.9%), yet with a slight worse constraint tolerance (2.5%) than the original OptLayer method (2.3%). Also, the initial utility of both of our proposed methods is significantly higher (92.4% and 92.2%) compared to OptLayer (86.1%), as initially, they use the SafeFallback policy π^{safe} itself (97.2%) – due to surpassing the set threshold h_{safe} in algorithm 1. All safety layer methods are, as intended, significantly safer than the unconstrained *vanilla* TD3 benchmark, which has an initial NMAE of 56.5% and reaches 8.1% under the consequence of the $L_{comfort}^t$ term in Equation 10g. The higher constraint tolerance of the original SafeFallback method itself can be explained by the fact that it is not capable of handling equality constraints [5] (as otherwise the constraint *check* would seldom be passed). The constraint tolerances of the other safety layer methods are in the same order of magnitude, both before and after training – all in line with the NMAE of the constraint functions themselves (Table 2 and Figure 6).

Table 5. 5-run average policy performance before any training

EMS algorithm	Objective value		Constraint tolerance	
	absolute	relative	NMAE	NSUM
Unsafe Random	-14,223	35.7%	56.5%	146.0%
OptLayer Random	-5,900	86.1%	3.1%	8.0%
SafeFallback Random	-5,331	95.3%	2.7%	7.0%
SafeFallback (π^{safe})	-5,228	97.2%	2.4%	6.3%
OptLayerPolicy Random	-5,499	92.4%	2.9%	7.4%
GreyOptLayerPolicy Random	-5,512	92.2%	2.4%	6.3%

**Figure 4.** 5-run average learning curves with a training budget of 10 years worth of time steps per run (i.e. 350,400 time steps per run). Note that the y-axis is zoomed in (see [Figure B.1](#) in [Appendix B](#) for the zoomed-out version)

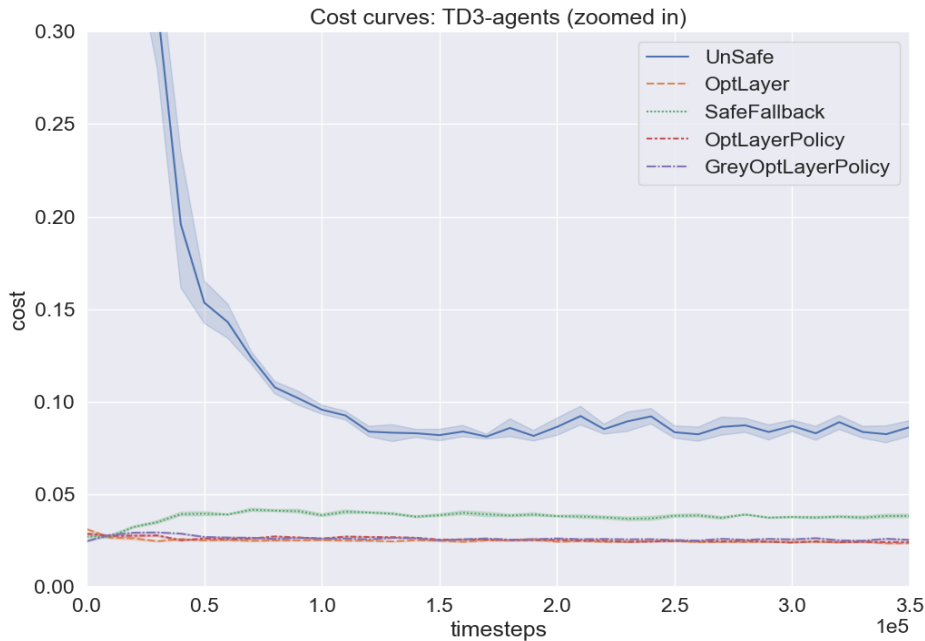
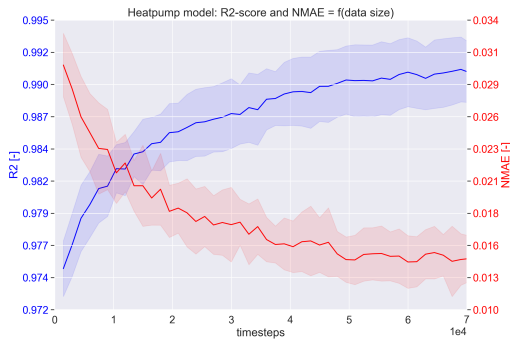
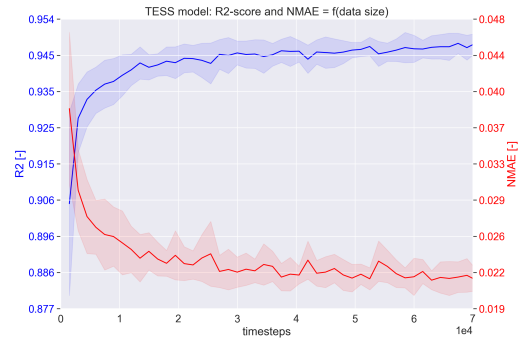


Figure 5. 5-run average cost curve (i.e. normalized mean absolute error) with a training budget of 10 years worth of time steps per run (i.e. 350,400 time steps per run). Note that the y-axis is zoomed in (see [Figure B.2](#) in [Appendix B](#) for the zoomed-out version).

The learning curves of the TD3 agents are presented in [Figure 4](#). The initial (at time step 0) and final (at time step 354,400) results are the values reported in [Table 4](#) and [Table 5](#) respectively. We observe a steep initial learning rate (except for the original `SafeFallback` method), low variance, and a stable performance with an increasing amount of interactions with its environment. As already reported here above, we observe that our `OptLayerPolicy` and `GreyOptLayerPolicy` have a significantly higher initial utility compared to the original `OptLayer` and *vanilla* `Unsafe` approach. This, again, is due to the additional *a priori* expert knowledge in the form of the safe fallback policy π^{safe} and in the form of the constraint functions themselves (which is also true for the `OptLayer` approach compared to the unsafe *vanilla* RL agent). The `GreyOptLayerPolicy` algorithm surpasses `OptLayerPolicy` just after $\approx 20,000$ time steps (7 months) and `OptLayer` after $\approx 50,000$ time steps (17 months). The original `SafeFallback` method gets quickly surpassed by all other safety layer methods.



(a) Heat pump: $Q_{hp}^t = f(a_{hp}^t, Q_{hp}^{t-1})$ with [25,20,20,10] hidden neurons using ReLU activation functions



(b) Thermal energy storage system: $Q_{tess}^t = f(a_{tess}^t, SOC_{tess}^t, Q_{tess}^{t-1}, Q_{demand}^{t-1})$ with [15,10,10,10] hidden neurons using ReLU activation functions

Figure 6. Safety layer: total (nominal and unknown component, i.e. Equation 7) modelling metrics for the first 2 years' worth of data, while interacting with the environment. The Mean Absolute Error is normalized by range (right-hand y-axis).

The cost curves of the TD3 agents are presented in Figure 5. The initial (at time step 0) and final (at time step 354,400) results are the values reported in Table 4 and Table 5 respectively. We observe a relatively constant constraint tolerance when using a safety layer (even though, in the GreyOptLayerPolicy method, the constraint functions themselves also improve – as can be seen in Figure 6), which can be explained by the fact that energy fulfilment is conflicting with the energy cost minimization objective (i.e. without a thermal demand fulfilment constraint, all thermal production would be turned off as these technical units consume and thus cost energy). The energy-minimizing RL agents, therefore, push the multi-energy system to the respective limit of their energy balancing constraints (and thus exploit the nominal and remaining modelling error of the constraint functions themselves). The unconstrained *vanilla* TD3 benchmark does have a significant drop in its constraint tolerance under the consequence of the $L_{comfort}^t$ term in Equation 10g (which has far less impact when using a safety layer). As mentioned before, the higher constraint tolerance of the original SafeFallback method itself can be explained by the fact that it is not capable of handling equality constraints (as otherwise the constraint *check* would seldom be passed), which forces a relaxation of the thermal energy balance constraint.

6. Conclusion

This paper presented a novel model-free safe RL approach of the following *combined* characteristics: (i) providing hard-constraints satisfaction guarantees (ii) while decoupled from the RL (as a Markov Decision Process) formulation, (iii) both during training a (near) optimal policy (which involves exploratory and exploitative steps) as well as during the deployment of any policy (e.g. random agents or offline pre-trained RL agents) and (iv) this while learning uncertain constraint components and safely improving the policy with high sample efficiency, and (v) starting from an increased initial utility, to (vi) demonstrate for the energy management of multi-energy systems.

We conclude that, while special attention is required to introduce surrogate functions into the optimization problem, the `GreyOptLayerPolicy` method is the most advantageous due to both the increase of its initial utility *and* the ability to self-improve its constraints, leading to better policies. Finally, we propose the following directions for future work:

- Robustness of the RL-based energy management systems under faulty and noisy measurements/observations and utilizing *online* hyperparameter optimization methods (i.e. that the hyperparameters are tuned during online training).
- Reduce computational complexity of the safety layer when using surrogate constraint functions or parameters so that more detailed function approximation architectures can be used (e.g. more neurons and layers in an ANN).
- Verification of the proposed methods in a controlled lab environment.

7. Acknowledgement

This work has been supported in equal parts by ABB n.v. and Flemish Agency for Innovation and Entrepreneurship (VLAIO) grant HBC.2019.2613.

CRediT authorship contribution statement

Glenn Ceusters: Conceptualization, Methodology, Software, Validation, Formal analysis, Resources, Data curation, Writing - original draft, Visualization, Funding acquisition; **Muhammad Andy Putratama:** Conceptualization, Writing - review and editing, Supervision; **Rüdiger Franke:** Supervision; **Ann Nowé:** Writing - review and editing, Supervision; **Maarten Messagie:** Supervision.

Appendix A Simulations visualization

In this section, we show a time series visualization sample (a week) of the found control policies. The plots, and their description, of the benchmarks (i.e. UnSafe, OptLayer and SafeFallback) are not repeated here as they can be found in [Ceusters *et al.* \[5\]](#). Our first observation is that the initial policy of both OptLayerPolicy ([Figure A.1](#)) and GreyOptLayerPolicy ([Figure A.3](#)) are very similar. This is, at this stage, they have the same (nominal) constraints, and occasionally the predicted actions, \tilde{a} , are close enough to the feasible solution space (calculated using [Equation 6](#)) so that they are minimally corrected and thus don't surpass the given threshold h_{safe} . As intended, most of the time, this threshold is surpassed and thus the safe fallback policy π_{safe} is used – in accordance with [algorithm 1](#).

When analysing the policies of the TD3 agents, after safely training them (i.e. [Figure A.2](#) and [Figure A.4](#)), we observe that both continue to have a low constraint tolerance, as expected. However, the GreyOptLayerPolicy policy is slightly better at using the heat pump when electricity prices are low, producing electricity with the CHP and charging the TESS simultaneously when electricity prices are high and vice versa. Hence, it is better at minimizing energy costs. In both cases, however, the BESS is underutilized, i.e. it fails to learn to charge the BESS when electricity prices are low and discharging the BESS when prices are high. This underutilization of the BESS was reported in previous work as well (e.g. [Ceusters *et al.* \[4\]](#) and [Ceusters *et al.*\[5\]](#)), which will require revisiting the state-space formulation ([Equation 10a](#)) and the consideration of specific reward shaping in [Equation 10g](#).

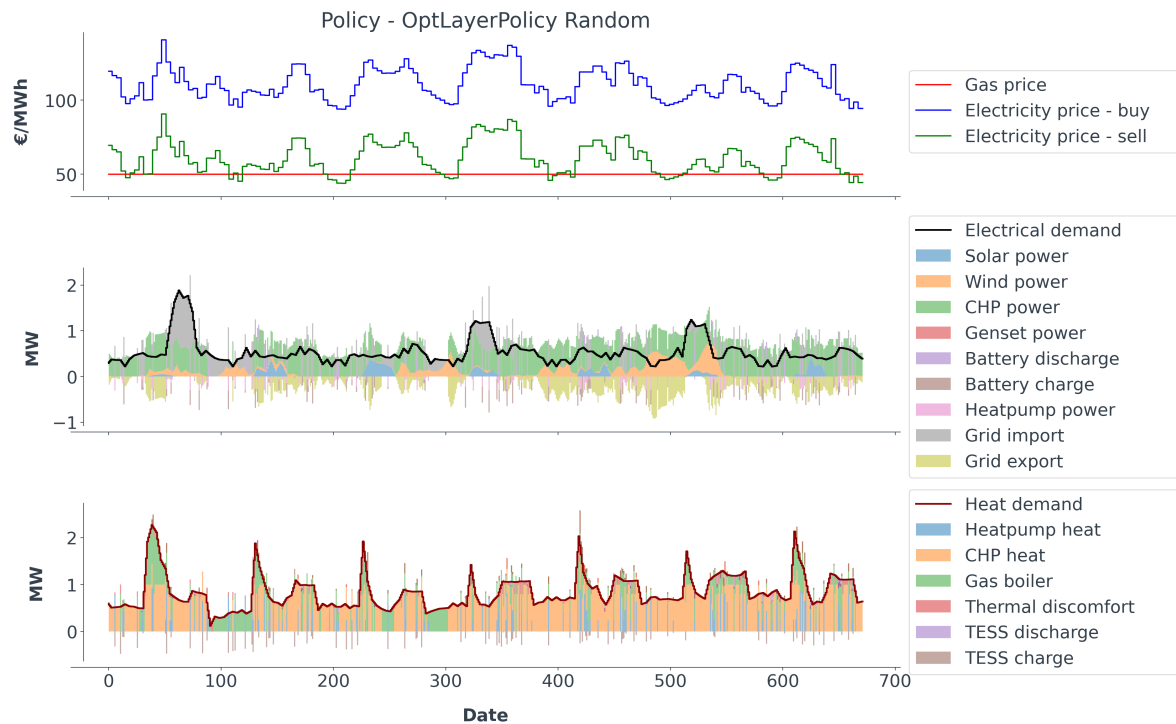


Figure A.1. Policy visualization: OptLayerPolicy random (or TD3 before training)

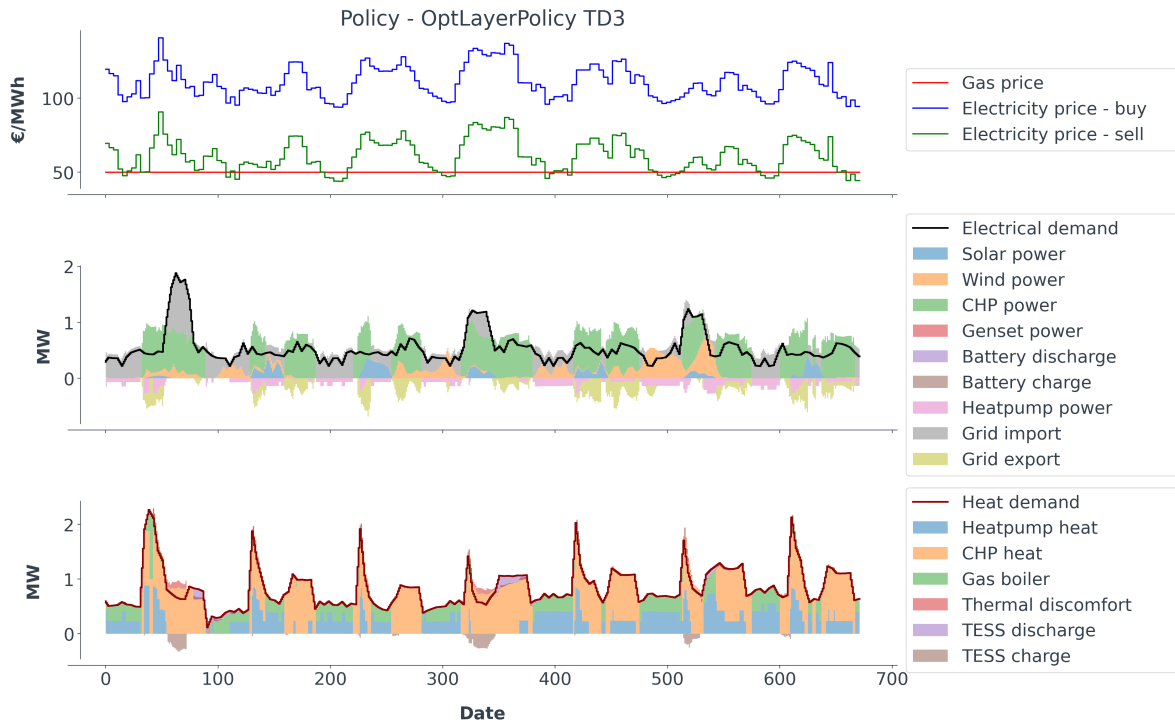


Figure A.2. Policy visualization: OptLayerPolicy TD3 (after safe training)

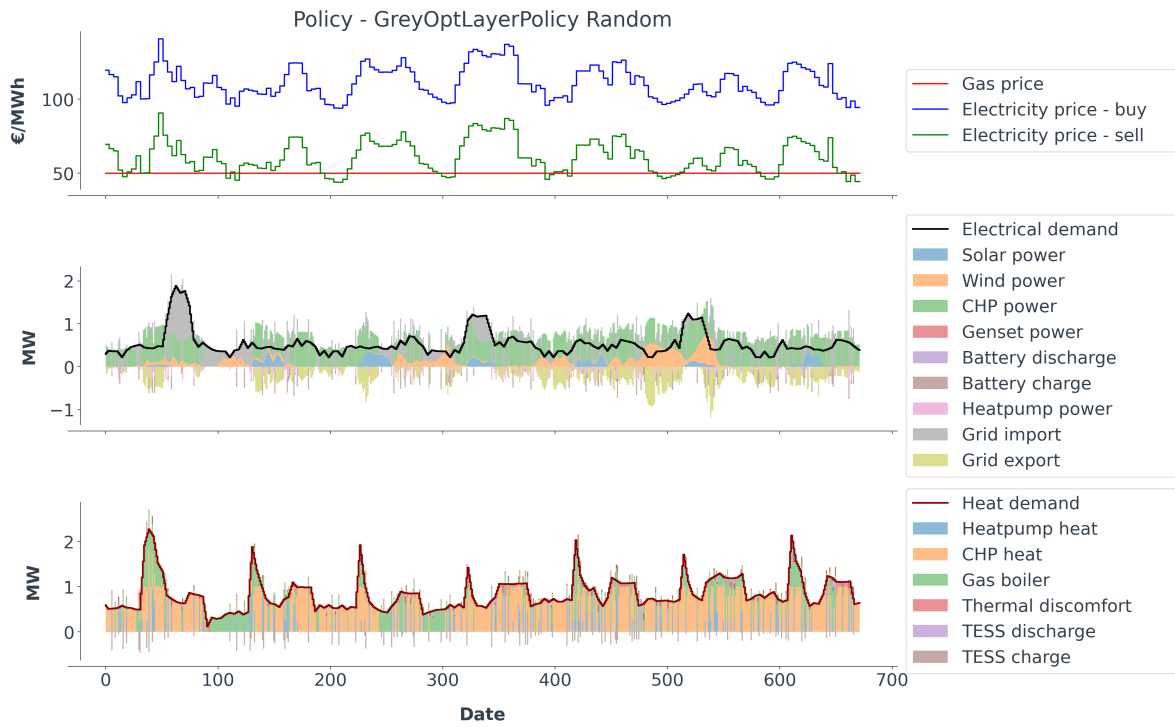


Figure A.3. Policy visualization: GreyOptLayerPolicy random (or TD3 before training)

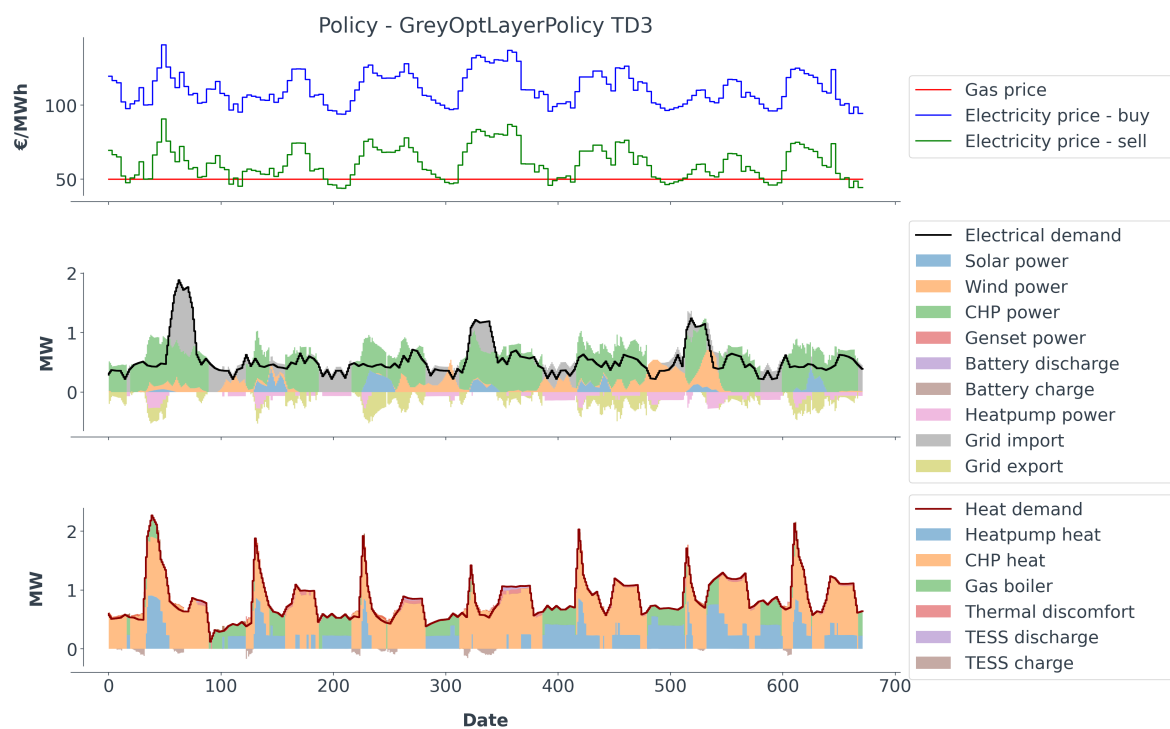


Figure A.4. Policy visualization: GreyOptLayerPolicy TD3 (after safe training)

Appendix B Learning and costs curves: zoomed out

This appendix shows the zoomed-out learning and costs curves of the TD3-agents so that all curves are fully visible, i.e. so that the UnSafe curves are visible for all time steps.

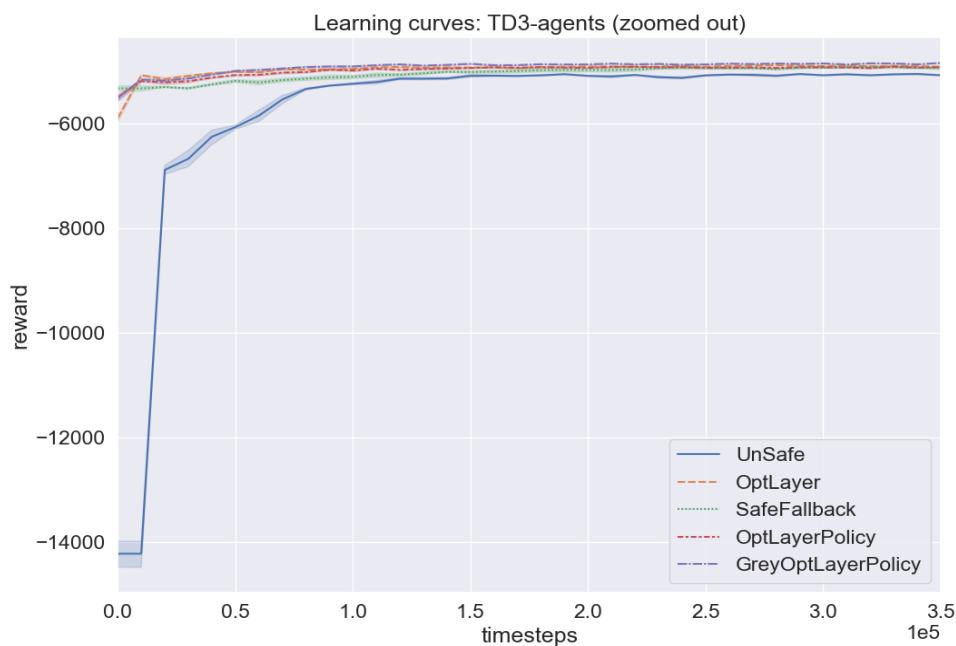


Figure B.1. 5-run average learning curves with a training budget of 10 years worth of time steps per run (i.e. 350,400 time steps per run). Note that the zoomed-in version is [Figure 4](#).

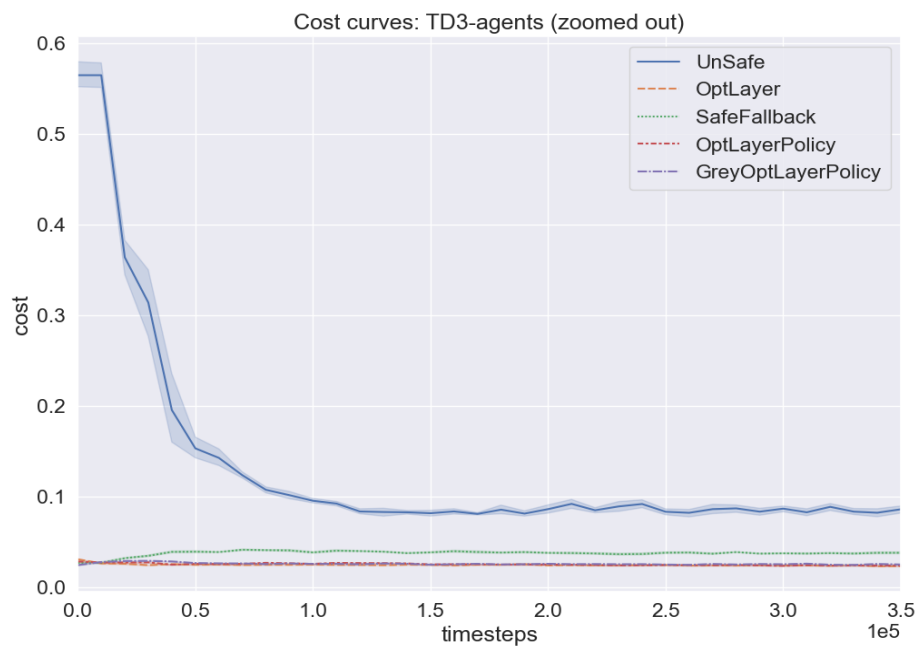


Figure B.2. 5-run average cost curve (i.e. normalized mean absolute error) with a training budget of 10 years worth of time steps per run (i.e. 350,400 time steps per run). Note that the zoomed-in version is [Figure 5](#).

Appendix C Pseudocode of TD3

Algorithm 2: Twin Delayed DDPG (TD3) [30]

- 1 Input: initial policy parameters θ , Q-function parameters ϕ_1, ϕ_2 , empty replay buffer \mathcal{D}
- 2 Set target parameters equal to main parameters $\theta_{\text{targ}} \leftarrow \theta, \theta_{\text{targ},1} \leftarrow \theta_1, \theta_{\text{targ},2} \leftarrow \theta_2$
- 3 **repeat**
- 4 Observe state s and select action $a = \text{clip}(\mu_\theta(s) + \epsilon, a_{\text{Low}}, a_{\text{High}})$, where $\epsilon \sim \mathcal{N}$
- 5 Execute a in the environment
- 6 Observe next state s' , reward r and done signal d to indicate whether s' is terminal
- 7 Store (s, a, r, s', d) in replay buffer \mathcal{D}
- 8 If s' is terminal, reset environment state
- 9 **if it's time to update then**
- 10 **for** j in range(however many updates) **do**
- 11 Randomly sample a batch of transitions, $B = \{(s, a, r, s', d)\}$ from \mathcal{D}
- 12 Compute target actions

$$a'(s') = \text{clip}(\mu_{\theta_{\text{targ}}}(s') + \text{clip}(\epsilon, -c, c), a_{\text{Low}}, a_{\text{High}}), \quad \epsilon \sim \mathcal{N}(0, \sigma)$$

- 13 Compute targets

$$y(r, s', d) = r + \gamma(1 - d) \min_{i=1,2} Q_{\phi_{\text{targ},i}}(s', a'(s'))$$

- 14 Update Q-function by one step of gradient descent using

$$\nabla_{\phi_i} \frac{1}{|B|} \sum_{(s,a,r,s',d) \in B} (Q_{\phi_i}(s, a) - y(r, s', d))^2 \quad \text{for } i = 1, 2$$

- 15 **if** $j \bmod \text{policy_delay} = 0$ **then**
- 16 Update policy by one step of gradient ascent using

$$\nabla_{\theta} \frac{1}{|B|} \sum_{s \in B} Q_{\phi_1}(s, \mu_\theta(s))$$

- 17 Update target networks with

$$\begin{aligned} \phi_{\text{targ},i} &\leftarrow \rho \phi_{\text{targ},i} + (1 - \rho) \phi_i & \text{for } i = 1, 2 \\ \theta_{\text{targ}} &\leftarrow \rho \theta_{\text{targ}} + (1 - \rho) \theta \end{aligned}$$

- 18 **end if**
 - 19 **end for**
 - 20 **end if**
 - 21 **until** convergence
-

Appendix D Run-time statistics

The simulations are conducted on a local machine with an Intel® Core™ i5-8365U CPU @1.6GHz, 16 GB of Ram and an SSD. Over a yearly simulation, the following run-time statistics per simulated time-step (with a control horizon of 15 min) are observed.

Table D.1. Run-time statistics *after* training (i.e., pure policy execution)

Optimal controller	min	mean	std	max	total
Unsafe TD3	0,032 s	0,053 s	0,009 s	0,270 s	1.858 s
Unsafe Random	0,029 s	0,046 s	0,008 s	0,124 s	1.630 s
OptLayer TD3	0,211 s	0,291 s	0,036 s	0,976 s	10.204 s
OptLayer Random	0,177 s	0,254 s	0,042 s	2,256 s	8.917 s
SafeFallback TD3	0,042 s	0,061 s	0,007 s	0,189 s	2.134 s
SafeFallback Random	0,038 s	0,046 s	0,007 s	0,492 s	1.608 s
SafeFallback (π^{safe})	0,038 s	0,050 s	0,010 s	0,190 s	1.738 s
OptLayerPolicy TD3	0,202 s	0,257 s	0,023 s	1,259 s	9.008 s
OptLayerPolicy Random	0,177 s	0,222 s	0,028 s	2,897 s	7.783 s
GreyOptLayerPolicy TD3	1,442 s	1,944 s	0,378 s	10,066 s	68.106 s
GreyOptLayerPolicy Random	1,436 s	1,918 s	0,361 s	6,504 s	67.222 s

The maximum run-time per time-step never exceeds the control horizon of 15 minutes, as this otherwise would be considered impractical with the given hardware. We observe that both the `Unsafe` and `SafeFallback` approaches have the fastest run-time, as they don't have a mathematical program to solve. However, we have argued that using a *vanilla* RL agent (i.e. without any safety measures) is not realistic in safety-critical environments and is here given for completeness only. We have also argued that the `SafeFallback` approach is not capable of handling equality constraints, which resulted in a higher constraint tolerance and is seen as a major drawback of the original method. As expected, the run-time of the `OptLayer` and `OptLayerPolicy` approaches are in the same order of magnitude as both involve solving a mixed-integer quadratic program (MIQP) in order to compute the closest feasible action and the distance of the predicted action, \tilde{a} , to the feasible solution space. Finally, we observe that the `GreyOptLayerPolicy` approach has the slowest run-time, which in turn hurts its scalability. This is due to the fact that the surrogate functions used to learn the uncertain constraint components are converted within the gradient descent optimization framework of GEKKO to allow for an exact solution. As proposed in future work, other surrogate function integration methods should be explored to reduce computational complexity.

References

1. Fabrizio, E.; Filippi, M.; Virgone, J. Trade-off between environmental and economic objectives in the optimization of multi-energy systems. *Building Simulation* 2009 2:1 **2009**, 2, 29–40. doi:10.1007/S12273-009-9202-4.
2. Engell, S. Feedback control for optimal process operation. *Journal of Process Control* **2007**, 17, 203–219. doi:10.1016/J.JPROCONT.2006.10.011.
3. Görges, D. Relations between Model Predictive Control and Reinforcement Learning. *IFAC-PapersOnLine* **2017**, 50, 4920–4928. doi:10.1016/j.ifacol.2017.08.747.
4. Ceusters, G.; Rodríguez, R.C.; García, A.B.; Franke, R.; Deconinck, G.; Helsen, L.; Nowé, A.; Messagie, M.; Camargo, L.R. Model-predictive control and reinforcement learning in multi-energy system case studies. *Applied Energy* **2021**, 303, 117634. doi:10.1016/j.apenergy.2021.117634.
5. Ceusters, G.; Camargo, L.R.; Franke, R.; Nowé, A.; Messagie, M. Safe reinforcement learning for multi-energy management systems with known constraint functions. *Energy and AI* **2023**, 12, 100227. doi:10.1016/J.EGYAI.2022.100227.
6. Pham, T.H.; De Magistris, G.; Tachibana, R. OptLayer - Practical Constrained Optimization for Deep Reinforcement Learning in the Real World. *Proceedings - IEEE International Conference on Robotics and Automation* **2018**, pp. 6236–6243. doi:10.1109/ICRA.2018.8460547.

7. Cao, D.; Hu, W.; Zhao, J.; Zhang, G.; Zhang, B.; Liu, Z.; Chen, Z.; Blaabjerg, F. Reinforcement Learning and Its Applications in Modern Power and Energy Systems: A Review. *Journal of Modern Power Systems and Clean Energy* **2020**, *8*, 1029–1042. doi:10.35833/MPCE.2020.000552.
8. Yang, T.; Zhao, L.; Li, W.; Zomaya, A.Y. Reinforcement learning in sustainable energy and electric systems: a survey. *Annual Reviews in Control* **2020**, *49*, 145–163. doi:10.1016/J.ARCONTROL.2020.03.001.
9. Perera, A.T.; Kamalaruban, P. Applications of reinforcement learning in energy systems. *Renewable and Sustainable Energy Reviews* **2021**, *137*, 110618. doi:10.1016/J.RSER.2020.110618.
10. Zhou, Y. Advances of machine learning in multi-energy district communities– mechanisms, applications and perspectives. *Energy and AI* **2022**, *10*, 100187. doi:10.1016/J.EGYAI.2022.100187.
11. Petrusev, A.; Putratama, M.A.; Rigo-Mariani, R.; Debusschere, V.; Reignier, P.; Hadjsaid, N. Reinforcement learning for robust voltage control in distribution grids under uncertainties. *Sustainable Energy, Grids and Networks* **2023**, *33*, 100959. doi:10.1016/J.SEGAN.2022.100959.
12. Zhou, Y.; Ma, Z.; Zhang, J.; Zou, S. Data-driven stochastic energy management of multi energy system using deep reinforcement learning. *Energy* **2022**, *261*, 125187. doi:10.1016/J.ENERGY.2022.125187.
13. Pu, Y.; Wang, S.; Yang, R.; Yao, X.; Li, B. Decomposed Soft Actor-Critic Method for Cooperative Multi-Agent Reinforcement Learning. *arXiv* **2021**.
14. Zhu, D.; Yang, B.; Liu, Y.; Wang, Z.; Ma, K.; Guan, X. Energy Management Based on Multi-Agent Deep Reinforcement Learning for A Multi-Energy Industrial Park. *Applied Energy* **2022**, *311*, 118636. doi:10.1016/j.apenergy.2022.118636.
15. Ahrarinouri, M.; Rastegar, M.; Karami, K.; Seifi, A.R. Distributed reinforcement learning energy management approach in multiple residential energy hubs. *Sustainable Energy, Grids and Networks* **2022**, *32*, 100795. doi:10.1016/J.SEGAN.2022.100795.
16. Jendoubi, I.; Bouffard, F. Data-driven sustainable distributed energy resources' control based on multi-agent deep reinforcement learning. *Sustainable Energy, Grids and Networks* **2022**, *32*, 100919. doi:10.1016/J.SEGAN.2022.100919.
17. Sun, B.; Song, M.; Li, A.; Zou, N.; Pan, P.; Lu, X.; Yang, Q.; Zhang, H.; Kong, X. Multi-objective solution of optimal power flow based on TD3 deep reinforcement learning algorithm. *Sustainable Energy, Grids and Networks* **2023**, *34*, 101054. doi:10.1016/J.SEGAN.2023.101054.
18. Feng, J.; Wang, H.; Yang, Z.; Chen, Z.; Li, Y.; Yang, J.; Wang, K. Economic dispatch of industrial park considering uncertainty of renewable energy based on a deep reinforcement learning approach. *Sustainable Energy, Grids and Networks* **2023**, *34*, 101050. doi:10.1016/J.SEGAN.2023.101050.
19. Brunke, L.; Greeff, M.; Hall, A.W.; Yuan, Z.; Zhou, S.; Panerati, J.; Schoellig, A.P. Safe Learning in Robotics: From Learning-Based Control to Safe Reinforcement Learning. *Annual Review of Control, Robotics, and Autonomous Systems* **2021**, *5*. doi:10.1146/annurev-control-042920-020211.
20. McKinnon, C.D.; Schoellig, A.P. Context-aware Cost Shaping to Reduce the Impact of Model Error in Receding Horizon Control. *Proceedings - IEEE International Conference on Robotics and Automation* **2020**, pp. 2386–2392. doi:10.1109/ICRA40945.2020.9197521.
21. Bharadhwaj, H.; Kumar, A.; Rhinehart, N.; Levine, S.; Shkurti, F.; Garg, A. Conservative Safety Critics for Exploration. *International Conference on Learning Representations*, 2021.
22. Lopez, B.T.; Slotine, J.J.E.; How, J.P. Robust Adaptive Control Barrier Functions: An Adaptive and Data-Driven Approach to Safety. *IEEE Control Systems Letters* **2021**, *5*, 1031–1036. doi:10.1109/LCSYS.2020.3005923.
23. Gunnell, L.L.; Manwaring, K.; Lu, X.; Reynolds, J.; Vienna, J.; Hedengren, J. Machine Learning with Gradient-Based Optimization of Nuclear Waste Vitrification with Uncertainties and Constraints. *Processes* **2022**, *10*, 2365. doi:10.3390/pr10112365.
24. Mattsson, S.E.; Elmqvist, H.; Otter, M. Physical system modeling with Modelica. *Control Engineering Practice*. Pergamon, 1998, Vol. 6, pp. 501–510. doi:10.1016/S0967-0661(98)00047-1.
25. Gräber, M.; Fritzsche, J.; Tegethoff, W. From system model to optimal control - A tool chain for the efficient solution of optimal control problems. *Proceedings of the 12th International Modelica Conference, Prague, Czech Republic, May 15-17, 2017*. Linköping University Electronic Press, 2017, Vol. 132, pp. 249–254. doi:10.3384/ecp17132249.

26. Brockman, G.; Cheung, V.; Pettersson, L.; Schneider, J.; Schulman, J.; Tang, J.; Zaremba, W. OpenAI Gym. *arxiv* **2016**.
27. Beal, L.; Hill, D.; Martin, R.; Hedengren, J. GEKKO Optimization Suite. *Processes* **2018**, *6*, 106. doi:10.3390/pr6080106.
28. Andersson, C.; Akesson, J.; Fuhrer, C. PyFMI: A Python Package for Simulation of Coupled Dynamic Models with the Functional Mock-up Interface. Technical Report 2, Lund University, 2016.
29. Raffin, A.; Hill, A.; Gleave, A.; Kanervisto, A.; Ernestus, M.; Dormann, N. Stable-Baselines3: Reliable Reinforcement Learning Implementations. *Journal of Machine Learning Research* **2021**, *22*, 1–8.
30. OpenAI. Twin Delayed DDPG — Spinning Up documentation, 2020.